ChinaXiv合作期刊

Synergistic effects of multiple driving factors on the runoff variations in the Yellow River Basin, China

WANG Junjie[1], SHI Bing[1*], ZHAO Enjin[1,2], CHEN Xuguang[1*], YANG Shaopeng[3]

[1] College of Engineering, Ocean University of China, Qingdao 266100, China;
[2] Hubei Key Laboratory of Marine Geological Resources, China University of Geosciences, Wuhan 430074, China;
[3] College of Ocean Science and Engineering, Shandong University of Science and Technology, Qingdao 266590, China

chinaXiv:202109.00013v1

Abstract: River runoff plays an important role in watershed ecosystems and human survival, and it is controlled by multiple environmental factors. However, the synergistic effects of various large-scale circulation factors and meteorological factors on the runoff on different time-frequency scales have rarely been explored. In light of this, the underlying mechanism of the synergistic effects of the different environmental factors on the runoff variations was investigated in the Yellow River Basin of China during the period 1950–2019 using the bivariate wavelet coherence (WTC) and multiple wavelet coherence (MWC) methods. First, the continuous wavelet transform (CWT) method was used to analyze the multiscale characteristics of the runoff. The results of the CWT indicate that the runoff exhibited significant continuous or discontinuous annual and semiannual oscillations during the study period. Scattered inter-annual time scales were also observed for the runoff in the Yellow River Basin. The meteorological factors better explained the runoff variations on seasonal and annual time scales. The average wavelet coherence (AWC) and the percent area of the significant coherence (PASC) between the runoff and individual meteorological factors were 0.454 and 19.89%, respectively. The circulation factors mainly regulated the runoff on the inter-annual and decadal time scales with more complicated phase relationships due to their indirect effects on the runoff. The AWC and PASC between the runoff and individual circulation factors were 0.359 and 7.31%, respectively. The MWC analysis revealed that the synergistic effects of multiple factors should be taken into consideration to explain the multiscale characteristic variations of the runoff. The AWC or MWC ranges were 0.320–0.560, 0.617–0.755, and 0.819–0.884 for the combinations of one, two, and three circulation and meteorological factors, respectively. The PASC ranges were 3.53%–33.77%, 12.93%–36.90%, and 20.67%–39.34% for the combinations one, two, and three driving factors, respectively. The combinations of precipitation, evapotranspiration (or the number of rainy days), and the Arctic Oscillation performed well in explaining the variability in the runoff on all time scales, and the average MWC and PASC were 0.847 and 28.79%, respectively. These findings are of great significance for improving our understanding of hydro-climate interactions and water resources prediction in the Yellow River Basin.

Keywords: synergistic effects; precipitation; runoff variations; atmospheric circulations; multiple wavelet coherence; Yellow River Basin

*Corresponding authors: SHI Bing (E-mail: sediment@ouc.edu.cn); CHEN Xuguang (Email: chenxuguang1984@ouc.edu.cn)
Received 2021-02-22; revised 2021-07-27; accepted 2021-07-29
© Xinjiang Institute of Ecology and Geography, Chinese Academy of Sciences, Science Press and Springer-Verlag GmbH Germany, part of Springer Nature 2021

ChinaXiv合作期刊

chinaXiv:202109.00013v1

1 Introduction

As one of the most important sources of fresh water on land, the river runoff plays a vital role in human survival and health, biological diversity, economic development, and social stability (Arthington et al., 2010; Li et al., 2017a). The streamflow is determined by multiple driving factors, mainly including meteorological factors (e.g., precipitation, temperature, and evapotranspiration), large-scale global atmospheric circulation factors (e.g., the Arctic Oscillation (AO), North Atlantic Oscillation (NAO), Pacific Decadal Oscillation (PDO), and El Niño-Southern Oscillation (ENSO)), and human activities. The responses of the runoff to different factors vary on different time scales (Labat, 2008; Su et al., 2017). Precipitation plays a dominant role in the long-term trend and inter-annual variability of the global runoff (Piao et al., 2007; Gerten et al., 2008). Furthermore, precipitation trends have been found to be spatially consistent with streamflow trends in observations (Xu et al., 2010), climate model simulations (Yang et al., 2019; Wu et al., 2020), and land surface models (Piao et al., 2007) in most regions. Evapotranspiration also plays a major role in controlling the evolution and cycling of the runoff (Wine and Zou, 2012; Huo et al., 2020). The rising temperature will not only lead to an increase in evapotranspiration, but also accelerate the melting of ice and snow (Niedzielski et al., 2019; Notarnicola, 2020). Moreover, after the permafrost melting caused by the increase in temperature, the infiltration capacity of the soil will be enhanced, which will result in complex changes in the runoff (Li et al., 2012).

Therefore, numerous previous studies have focused on the response relationships between the runoff and various meteorological factors worldwide (Shen et al., 2017; Chen et al., 2019; Chu et al., 2019; Wu et al., 2020). These studies have also reported that the response relationships between the runoff and various climate variables exhibit significant asymmetrical characteristics and nonlinear variations. For example, Shen et al. (2017) evaluated the impacts of various climatic factors on the runoff changes in 224 catchments in China based on a Budyko-type equation, and found that the precipitation depth can explain the runoff increase better in almost every basin. Chen et al. (2019) studied the regional asymmetric effect of the daily extreme temperature on the runoff variations in the Yellow River Basin (YRB) of China using the variable infiltration capacity model, and their results showed that the relationships between the runoff and both the highest and lowest temperature are upward parabolic functions. Chu et al. (2019) investigated the correlations and lag or lead times between the runoff and climate variables (precipitation, temperature, and evapotranspiration) through cross-correlation functions and wavelet coherence in the source area of the YRB, and their results revealed that the runoff is mainly controlled by precipitation and temperature on various timescales with certain time lags. Consequently, analyses of the effects of different meteorological factors on the nonlinear behavior and multiscale characteristics of the runoff must consider the combined influence of multiple complex driving factors. However, the aforementioned studies and most previous studies have mainly focused on the individual effects of single factors and cannot fully reflect the synergistic effects of multiple factors on the runoff variations.

In addition, the terrestrial runoff cycling is an important component of the hydrological cycle and is controlled by complex atmosphere-ocean-land interactions (Su et al., 2018; Liu et al., 2020). The atmosphere and oceans possess large heat capacities and convey a great deal of moisture in the climate system (Sun et al., 2016; Su et al., 2018). Fluctuations in the teleconnections caused by differences in the sea level pressure and/or sea surface temperature (SST) play a crucial role in regulating the regional and global water cycles (Nalley et al., 2019). Moreover, the large-scale circulation factors reflect the natural phenomena of atmosphere-ocean oscillations. The indices of circulation factors, such as the AO, Southern Oscillation Index (SOI), NAO, and PDO, are effective and convenient predictors of the runoff variations (Nijssen et al., 2001; Nalley et al., 2019).

Many studies have focused on the relationships between the runoff and large-scale atmospheric circulation factors worldwide. For instance, Labat (2010) analyzed the non-stationary relationships between the annual continental freshwater discharge and various large-scale

ChinaXiv合作期刊

chinaXiv:202109.00013v1

circulation factors (AO, NAO, PDO, SOI, and ENSO) using cross wavelet analysis and revealed that a temporal correlation generally exists within restricted intervals. Murgulet et al. (2017) statistically quantified the relationships of the runoff with the Atlantic Multidecadal Oscillation (AMO), ENSO, and PDO of southern Texas at the regional scale, and their results indicated that the runoff is strongly modulated by the PDO and ENSO during the warm and cold seasons. Cheng et al. (2019) investigated the relationships between the runoff variations and large-scale circulation factors (PDO, NAO, AO, AMO, and ENSO) using the wavelet coherence method and found that the monthly runoff has a significant resonance periodicity with various circulation factors. Evidently, the combined effects and scale-dependent relationships between the runoff and multiple circulation factors have rarely been explored. Moreover, the lack of attention to the synergistic effects of meteorological and circulation factors on the runoff variations is especially acute.

Streamflow is one of the most important components of the hydrological cycle. It exhibits highly complex non-linear and non-stationary characteristics and is affected by multiple combined factors (Nalley et al., 2019; Wu et al., 2020). Many previous studies have focused on the interaction relationships between the runoff and environmental factors, but these studies were mostly limited and ignored the combined effects of different driving factors (e.g., Wei et al., 2014; Montaldo and Sarigu, 2017). The bivariate wavelet coherence (WTC) method has been widely used to identify the interaction and phase relationships between two geological and/or hydrological variables on different timescales (Fang et al., 2015; Su et al., 2017; Wang et al., 2020). However, the WTC method can no longer be used when the purpose is to untangle the scale-specific and localized relationships involving more than two variables (Hu and Si, 2016). Therefore, Hu and Si (2016) proposed a new method, i.e., the multiple wavelet coherence (MWC) approach, based on the WTC. Furthermore, they also compared the MWC method with multiple spectral coherence and multivariate empirical mode decomposition methods and found that the MWC method outperforms the other methods owing to its ability to determine the localized multivariate and scale-specific relationships on non-stationary and nonlinear geophysical time series.

In the YRB, the synergistic effects of different driving factors on the runoff variations on different time-frequency scales have not been studied systematically. The main objective of this study is to investigate the individual and synergistic impacts of various large-scale circulation factors (AO, NAO, PDO, SOI, and SST) and meteorological factors (precipitation, temperature, evapotranspiration, and the number of rainy days) on the runoff variations in the YRB. First, the multiscale characteristics of the runoff at six selected hydrological stations (Tangnaihai, Shizuishan, Toudaoguai, Longmen, Huayuankou, and Lijin) on the Yellow River were analyzed using the continuous wavelet transform (CWT) method. Then, the scale-dependent and phase relationships between the runoff and individual environmental factors were explored using the WTC method. Finally, the synergistic effects of two to three driving factors on the multiscale characteristics of the runoff in different time-frequency domains were investigated using the MWC method. The results of this study could provide a theoretical basis for increasing our understanding of the internal mechanisms of the hydrological cycle and for achieving the sustainable use of the water resources in the YRB.

2 Study area and data collection

2.1 Study area

The Yellow River is the second-longest river in China, with a total length of 5464 km (Fig. 1). It originates in the Bayankala Mountains on the Qinghai-Tibet Plateau. The catchment area of the YRB (95°53′–119°05′E, 32°10′–41°50′N) is 0.795×10^6 km^2. It crosses the Loess Plateau and the North China Plain, and eventually empties into the Bohai Sea. The YRB has highly significant spatial variations in climate, topography, land use, and other aspects. In winter, the YRB is easily controlled by the polar cold air mass, with prevailing northwest winds and less precipitation. In summer, the YRB is mainly affected by the subtropical high-pressure in the western Pacific, with

ChinaXiv合作期刊

more precipitation (Wu et al., 2013). The annual precipitation in the YRB is about 450 mm, and it is unequally distributed throughout the year and geographically throughout the river basin. About 70% of the total annual precipitation occurs in the flood season (from June to September).

The Yellow River is famous for its extraordinarily high sediment load. The mean annual sediment load at the Tongguan hydrological station was 9.8×10^8 t from 1950 to 2014 (Shi et al., 2017). Since middle reaches of the Yellow River cross the Loess Plateau, where soil erosion is severe, the Loess Plateau is a major source (nearly 90%) of the sediment carried by the Yellow River (Wang et al., 2016). After the 1970s, a series of large-scale soil and water conservation measures were implemented on the Loess Plateau, weakening the erosion ability of rainstorms and dramatically decreasing the sediment load of the Yellow River (Peng et al., 2010). Under the influences of both climate change and human activities, the streamflow in the YRB declined significantly in the mid-1980s because of reservoir construction, water abstraction, and water and soil conservation measures (Liu et al., 2012). The sketch map of the YRB and its elevation are shown in Figure 1.

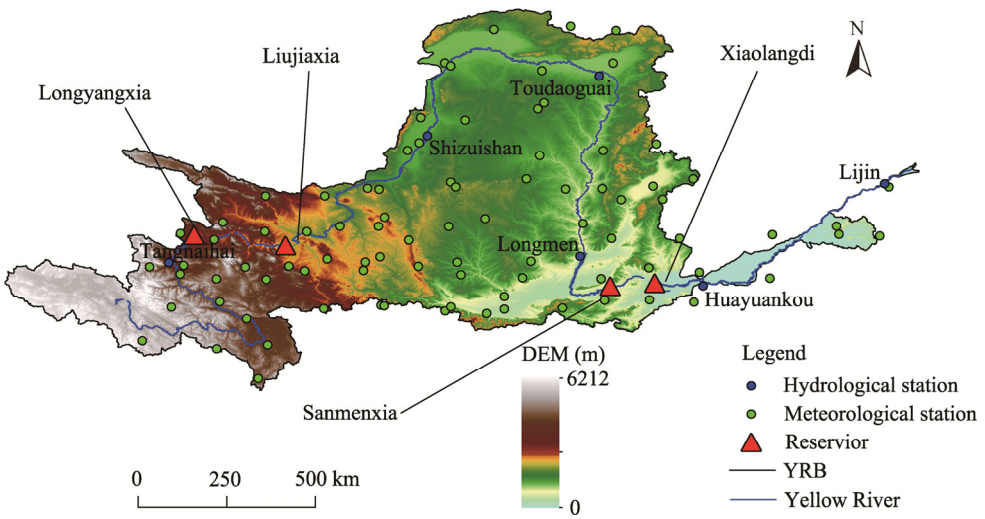

Fig. 1 Sketch map of the Yellow River Basin (YRB). DEM, digital elevation model.

2.2 Data collection

2.2.1 Streamflow data

The data used in this study consist of monthly runoff data from six control hydrological stations (Tangnaihai, Shizuishan, Toudaoguai, Longmen, Huayuankou, and Lijin) on the mainstream of the Yellow River. The data were mainly obtained from the Yellow River Conservancy Commission of the Ministry of Water Resources, China (period of 1950–2000), and the Yellow River Sediment Bulletin (Yellow River Conservancy Commission of the Ministry of Water Resources, 2001–2019). The dataset underwent strict review for correctness before its release, so the quality of the data is guaranteed. The locations of the hydrological stations are shown in Figure 1, and more information about the stations is presented in Table 1.

2.2.2 Meteorological data

The monthly data for the precipitation, temperature, evapotranspiration, and number of rainy days from 78 meteorological stations (Fig. 1) during the period of 1950–2019 were obtained from the China Meteorological Center (http://data.cma.cn). It should be noted that the number of rainy days is defined as a day with a daily rainfall of 0.1 mm or more (>0.1 mm). In the study, the data for the meteorological factors used for the interaction analysis with the streamflow at the six hydrological stations were different. They were the mean values of the area upstream of the hydrological stations and were calculated using the Thiessen polygon method (Croley II and Hartmann, 1985).

chinaXiv:202109.00013v1

ChinaXiv合作期刊

Table 1 Information about the hydrological stations selected in this study

Station	Data period	Distance to estuary (km)	Catchment area ($\times10^4$ km^2)	Mean annual runoff ($\times10^8$ m^3)
TNH	1950–2019	3911	12.20	202.17
SZS	1950–2019	2815	30.91	270.62
TDG	1956–2019	2146	36.79	207.86
LM	1950–2019	1269	49.76	258.97
HYK	1950–2019	768	73.00	368.83
LJ	1950–2019	104	75.19	293.80

Note: TNH, Tangnaihai; SZS, Shizuishan; TDG, Toudaoguai; LM, Longmen; HYK, Huayuankou; LJ, Lijin.

2.2.3 Circulation factor data

We investigated the relationships between the runoff and circulation factors, including the AO, NAO, PDO, SOI, and ENSO. The AO was used to describe the spatial distribution of the changes in the atmospheric anomalous phase between the Northern Hemisphere polar region and the mid-latitude sea level region (Thompson and Wallace, 1998; Thompson and Wallace, 2001). It regulates the circulation patterns in the middle and high latitude regions and thus the frequency and intensity of the weather events (Givati and Rosenfeld, 2013). The NAO index is defined as the difference between the normalized pressure at Gibraltar off southernmost Iberia and the normalized pressure in the south-western Iceland (Jones et al., 1997). The PDO represents a pattern of Pacific climate variability similar to the ENSO but not as extreme and with a longer period (Mantua et al., 1997). The PDO index is calculated from the monthly mean SST anomalies north of 20°N in the North Pacific (Hare and Mantua, 2000). The SOI is a measure of the atmospheric pressure gradient across the tropical Pacific. This version of the SOI is the difference between the normalized sea level pressure in Tahiti and Darwin, Australia (Hare and Mantua, 2000). The Nino3.4 index is the average SST anomaly in the region bounded by 5°N to 5°S and 170°W to 120°W (Trenberth, 1997). The monthly data for the AO, NAO, Nino3.4 index, and SOI were obtained from the National Weather Service Climate Prediction Centre (https://www.cpc.ncep.noaa.gov/). Further, the monthly PDO data were obtained from the National Oceanic and Atmosphere Administration (http://www.psl.noaa.gov/psd/).

3 Methodology

3.1 Continuous wavelet transform (CWT) method

The CWT method was used to decompose the time series of the runoff into different possible scales and to produce a wavelet power spectrum that could be used to test the periodic oscillation characteristics and variability. The choice of the mother wavelet function is crucial in wavelet analysis. The Morlet wavelet was used in this study, which has been widely adopted to analyze periodic oscillations in geophysical time series (Labat et al., 2000; Li et al., 2017b; Su et al., 2017). The Morlet wavelet is a nonorthogonal, complex function and is defined as:

$$\psi_0(\eta) = \pi^{-1/4} e^{i\,\omega_0\eta} e^{-\frac{1}{2}\eta^2}, \tag{1}$$

where η and ω_0 are the dimensionless time and frequency, respectively; $\psi_0(\eta)$ is the mother wavelet function; and i is a definite complex number, with a value of $\sqrt{-1}$. The value of ω_0 is commonly chosen to be 6 for the Morlet wavelet because this value provides a better balance between the time and frequency localization (Torrence and Compo, 1998; Grinsted et al., 2004).

Then, the CWT of a discrete time series X_t with a constant time step δt can be written as (Grinsted et al., 2004):

$$W_t^X(s) = \sum_{t'=0}^{N-1} X_{t'} \psi^* \left[\frac{(t'-t)\delta\, t}{s} \right], \tag{2}$$

where W_t^X is the wavelet transform of time series X at time index t; s is the wavelet scale; t is the time; $X_{t'}$ is the value of the time series X at time t'; N is the number of the time series; and the asterisk (*)

chinaXiv:202109.00013v1

ChinaXiv合作期刊

indicates the complex conjugate (Torrence and Compo, 1998). By varying the wavelet scale s and translating along the localized time index t, we can construct a picture depicting both the dominant modes of the variability and how these modes vary with time (Torrence and Compo, 1998; Jevrejeva et al., 2003). The data X is bounded in time, so the wavelet transform will be affected by edge effects.

3.2 Bivariate wavelet coherence (WTC)

Wavelet coherence is a useful method of quantifying the correlation between two non-stationary and nonlinear geophysical time series in the time-frequency domain. If X and Y are two time series, following the method of Torrence and Compo (1998), we can define the bivariate WTC as:

$$R_n^2(s,t) = \frac{\left|S(s^{-1}W_n^{XY}(s,t)\right|^2}{S(s^{-1}\left|W_n^X(s,t)\right|^2) \times S(s^{-1}\left|W_n^Y(s,t)\right|^2)}. \tag{3}$$

It should be noted that this definition closely resembles the traditional correlation coefficient, the coherence coefficient R_n^2, which takes a value between 0 and 1. W_n^{XY} is the cross-wavelet spectrum of X and Y; and W_n^X and W_n^Y are the CWT of X and Y, respectively. S is a smoothing operator that can be defined as:

$$S(W) = S_{\text{scale}}(S_{\text{time}}(W_n(s,t))), \tag{4}$$

where S_{scale} denotes smoothing along the wavelet scale; and S_{time} denotes smoothing in time. For the Morlet wavelet, the suitable smoothing operator is given by Torrence and Compo (1998):

$$S_{time}(W)\big|_s = (W_n(t,s) \times c_1^{\frac{-t^2}{2s^2}})\big|_s, \tag{5}$$

$$S_{\text{scale}}(W)\big|_t = (W_n(t,s) \times c_2 \prod(0.6s))\big|_s, \tag{6}$$

where W_n is the continuous wavelet transform of time series X or Y; c_1 and c_2 are the normalized constants; $\prod$ is a rectangle function; and the factor of 0.6 is the scale decorrelation length for the Morlet wavelet, which is determined empirically (Torrence and Compo, 1998).

3.3 Multiple wavelet coherence (MWC) method

Similar to the WTC method, the MWC method is also based on the auto- and cross-wavelet power spectra among the response variable (Y_t) and all of the predictor variables (X (X=X_1, X_2, ..., X_n)) at different scales and spatial locations. The auto- and cross-wavelet power spectra for the predictor variables (X (X=X_1, X_2, ..., X_n)) can be defined as (Koopmans, 1974):

$$W^{X,X}(s,\tau) = \begin{bmatrix} W^{X_1,X_1}(s,\tau) & W^{X_1,X_2}(s,\tau) & \cdots & W^{X_1,X_n}(s,\tau) \\ W^{X_2,X_1}(s,\tau) & W^{X_2,X_2}(s,\tau) & \cdots & W^{X_2,X_n}(s,\tau) \\ \vdots & \vdots & \vdots & \vdots \\ W^{X_n,X_1}(s,\tau) & W^{X_n,X_2}(s,\tau) & \cdots & W^{X_n,X_n}(s,\tau) \end{bmatrix}, \tag{7}$$

Where $W^{X_i,X_j}(s, \tau)$ represents the auto-wavelet power spectra (when i=j) or the cross-wavelet power spectra (when i≠j).

In addition, the matrix of the smoothed cross-wavelet power spectra between the predictor variables and the response variable can be written as:

$$W^{Y,X}(s,\tau) = \begin{bmatrix} W^{Y,X_1}(s,\tau) & W^{Y,X_2}(s,\tau) & \cdots & W^{Y,Xn}(s,\tau) \end{bmatrix}, \tag{8}$$

where $W^{Y,Xi}(s, \tau)$ is the smoothed cross-wavelet power spectra between the response variable Y and the predictor variable X_i.

In addition, the matrix of the smoothed cross-wavelet power spectra between the predictor variables and the response variable can be written as:

$$\rho_m^2(s,\tau) = \frac{W^{Y,X}(s,\tau)W^{Y,X}(s,\tau)^*}{W^{X,X}(s,\tau)W^{Y,Y}(s,\tau)}, \tag{9}$$

where $\rho_m^2(s, \tau)$ is the MWC at scale s and location τ; and $W^{Y,X}(s, \tau)^*$ is the complex conjugate of $W^{Y,X}(s, \tau)$. The 95% significance level of the CWT, WTC, and MWC were all calculated using the

chinaXiv:202109.00013v1

ChinaXiv合作期刊

Monte Carlo method (Torrence and Compo, 1998; Grinsted et al., 2004; Hu and Si, 2016). The average wavelet coherence (AWC or MWC) was calculated by averaging the wavelet coherence relative to the entire wavelet scale-location domain that produced in the WTC or MWC computation. The percent area of the significant coherence (PASC) was obtained by calculating the ratio of AWC or MWC values relative to the entire wavelet scale-location domain that passed the 95% significance level test (Hu and Si, 2016; Nalley et al., 2019). A greater AWC (or MWC) with a larger PASC indicates that more variations of the runoff can be explained by the environmental factors. The average coherence generally increases as the number of independent variables increases, but the PASC may not necessarily increase (Hu and Si, 2016). From a statistical point of view, the additional predicting environmental factor can only be considered to be significant when the PASC is increased by at least 5%.

4 Results

4.1 Multiscale characteristics of runoff

The CWT was applied to analyze the periodic characteristic variations in the discharge load of the different hydrological stations in the YRB. Figure 2 shows the wavelet power spectra of the runoff series in the YRB.

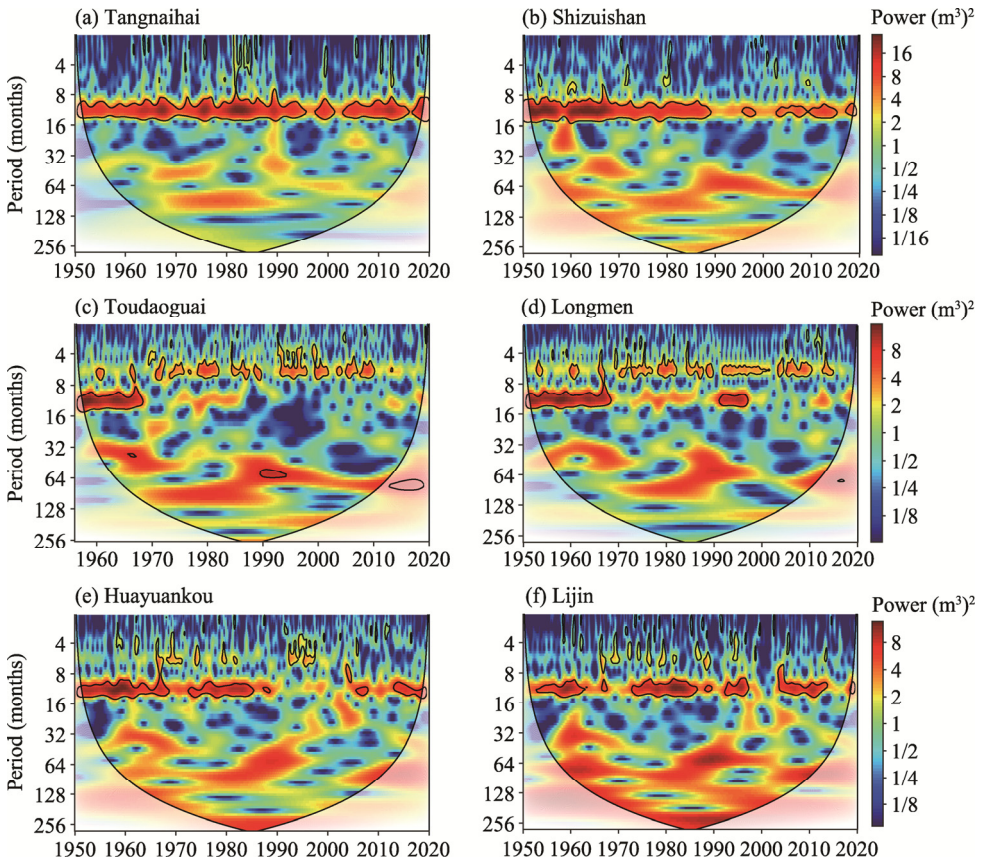

Fig. 2 Continuous wavelet spectra of the runoff time series at six hydrological stations. (a), Tangnaihai hydrological station; (b), Shizuishan hydrological station; (c) Toudaoguai hydrological station; (d), Longmen hydrological station; (e), Huayuankou hydrological station; (f), Lijin hydrological station.

The area surrounded by the thick black line indicates the time-frequency domain that reached the 95% significance level against red noise, and the pale area outside the thin black line is the cone of influence, in which the edge effects influence the interpretation. The value of the wavelet power can reflect the energy of the oscillation intensity, that is, the higher the energy of the

chinaXiv:202109.00013v1

ChinaXiv合作期刊

frequencies, the more significant the periodicities. It should be noted that the runoff at the various hydrological stations in the YRB exhibited similar periodic changes, and the annual oscillations' periodicity was significant at the Tangnaihai, Shizuishan, Huayuankou, and Lijin hydrological stations during the study period. Although some of the hydrological stations displayed a slight discontinuity in the annual oscillations, the difference was that the Toudaoguai and Longmen hydrological stations showed a significant half-year oscillation period. A significant annual periodicity was also observed at the Toudaoguai hydrological station from 1956 to 1968 and at the Longmen hydrological station from 1950 to 1970 and from 1992 to 1998. Furthermore, the wavelet power spectrum also revealed a relatively significant 3–10-a oscillation period from 1970 to 2000 at the Toudaoguai, Longmen, Huayuankou, and Lijin hydrological stations.

4.2 Relationships between the runoff and individual factors

The AWC or MWC and PASC were used to evaluate the effects of various factors on the multiscale characteristics of the runoff. Tables 2 and 3 show the AWC and PASC of the WTC between the runoff and individual environmental factors, respectively. The mean values of the AWC between the runoff and circulation factors and between the runoff and meteorological factors were 0.359 and 0.454, respectively (Table 2). The meteorological factors were the dominant drivers of the runoff variations, with the highest coherence at all six hydrological stations. Among the four meteorological factors (precipitation, temperature, evapotranspiration, and number of rainy days) we studied, precipitation and evapotranspiration were the most common influencing factors, with the highest coherence at two (Huayuankou and Lijin) and three hydrological stations (Tangnaihai, Shizuishan, and Toudaoguai), respectively. Temperature was the next most important factor, with the highest coherence for one station (Longmen). The highest AWC for the meteorological factors ranged from 0.439 to 0.560 across all of the stations, with an average highest AWC of 0.489. Moreover, among the five circulation factors, the AO was the most important influencing factor, with the highest AWC for all runoff series. The highest AWC for the circulation factors ranged from 0.378 to 0.420, with an average highest AWC of 0.397.

Table 2 Average wavelet coherence (AWC) between the runoff and individual circulation and meteorological factors at the six hydrological stations

Station	AO	NAO	PDO	SOI	SST	PRE	TEP	ET	WET
TNH	0.385	0.364	0.358	0.334	0.320	0.535	0.485	0.560	0.514
SZS	0.378	0.355	0.353	0.370	0.342	0.379	0.446	0.460	0.434
TDG	0.420	0.366	0.342	0.351	0.332	0.366	0.384	0.439	0.424
LM	0.412	0.357	0.342	0.363	0.354	0.461	0.476	0.420	0.472
HYK	0.403	0.337	0.348	0.356	0.345	0.537	0.423	0.407	0.473
LJ	0.383	0.338	0.372	0.350	0.345	0.462	0.452	0.446	0.435

Note: AO, Arctic Oscillation; NAO, North Atlantic Oscillation; PDO, Pacific Decadal Oscillation; SOI, Southern Oscillation Index; SST, sea surface temperature; PRE, precipitation; TEP, temperature; ET, evapotranspiration; WET, the number of rainy days.

Table 3 PASC values (%) for the wavelet coherence between the runoff and individual circulation and meteorological factors at the six hydrological stations

Station	AO	NAO	PDO	SOI	SST	PRE	TEP	ET	WET
TNH	11.44	5.91	12.47	4.53	3.64	33.77	26.85	28.33	33.14
SZS	9.18	5.82	9.27	9.24	4.41	15.36	21.10	19.43	19.48
TDG	15.03	5.84	6.70	5.14	4.22	11.77	10.07	15.96	12.12
LM	12.86	6.13	8.14	7.76	3.53	18.49	19.91	15.67	16.72
HYK	12.68	4.28	5.94	7.05	4.42	22.71	16.54	15.65	22.74
LJ	11.19	4.58	7.29	6.24	4.43	21.38	19.45	21.23	19.55

By comparing the AWC (Table 2) and PASC (Table 3), it was found that when the value of the AWC was the largest, the corresponding PASC may not be the largest. Moreover, the meteorological factors made a larger contribution to the multiscale characteristics of the runoff

chinaXiv:202109.00013v1

ChinaXiv合作期刊

chinaXiv:202109.00013v1

than the circulation factors. The largest PASC for the meteorological factors ranged from 15.96% to 33.77% across all of the hydrological stations, with an average largest PASC of 22.48%. Moreover, when considering the influence of an individual factor on the multiscale characteristics of the runoff, both precipitation and temperature were the dominant factors for two hydrological stations (Tangnaihai and Lijin for precipitation, and Shizuishan and Longmen for temperature). Evapotranspiration and the number of rainy days were respectively the dominant factor for one hydrological station (Toudaoguai and Huayuankou, respectively). The PASC values of the circulation factors were significantly lower than those of the meteorological factors, and the highest PASC of the circulation factors ranged from 9.27% to 15.03%, with an average of 12.25%. Among the five circulation factors we studied, the AO was the dominant factor and had the greatest effect on the multiscale characteristic of the runoff variations, with the highest PASC for four hydrological stations (Tangnaihai, Longmen, Huayuankou, and Lijin). The next most important circulation factor was the PDO, which had the highest PASC for two stations (Tangnaihai and Shizuishan).

Figure 3 shows the WTC results for the runoff and individual circulation factors that can best explain the multiscale characteristics of the runoff. The red area has a strong coherence, and the area surrounded by the thick black lines is the 95% significance level with a high PASC. Clearly, there was a strong coherence with complicated relative phase relationships between the runoff and PDO on the annual scale during the study period at the Tangnaihai hydrological station, especially from 1989 to 2019 (Fig. 3a). In addition, the coherence was strong at the Toudaoguai hydrological station on the 24- to 64-month timescale during 1950–2002 with a 95% significance level. Similar oscillation relationships occurred between the runoff and PDO at the Shizuishan hydrological station. Scattered semiannual and annual oscillation periods with the PDO were observed for the Shizuishan hydrological station, mainly during 1955–1965 and 1990–2015. For the semiannual oscillation period, the relative phase relationship between the runoff and PDO was mainly in anti-phase, while the phase relationship of the annual period was relatively complex. Moreover, the strong inter-annual oscillation periods (32–64 months) between the runoff and PDO were also observed during 1968–1980 (Fig. 3b).

The AO can best explain the multiscale characteristics of the runoff at the four hydrological stations located downstream of the Toudaoguai. However, the impacts of the AO on the runoff variations at different stations were somewhat different. At the Toudaoguai hydrological station, there were intermittent significant semiannual and annual oscillation periods between the runoff and AO. The oscillation periods of 32- to 64-month between the runoff and AO were particularly strong at the 95% confidence level, with a relative in-phase relationship from 1960 to 2000 (Fig. 3c). At the Longmen hydrological station, it was obvious that the coherence relationship between the runoff and AO was strong, and many domains were at the 95% significance level. In detail, for the 32- to 64-month oscillation periods, the runoff and AO had a strong coherence at the 95% significance level from 1960 to 2000, with the AO leading the runoff by approximately 45° (Fig. 3d). At the Huayuankou hydrological station, an annual oscillation period with a strong coherence was detected during 1960–1970, with the AO leading the runoff by 45°. Inter-annual oscillations (3- to 5-year) between the runoff and AO were observed at the Huayuankou hydrological station from 1960 to 2000 at a 95% significance level, with the AO leading the runoff by 45° (Fig. 3e). The coherence relationship between the runoff and AO at the Lijin hydrological station was similar to that at the Huayuankou hydrological station, mainly in the strong coherence domain of the time-frequency due to their similar geographical environments.

According to the WTC results for the runoff and individual meteorological factors that could best explain the multiscale characteristics of the runoff (Fig. 4), during the entire study period, there was a significant strong continuous coherence between the runoff and precipitation or temperature on the annual timescale at the Tangnaihai and Shizuishan hydrological stations. At the Tangnaihai and Shizuishan hydrological stations, the precipitation and temperature either led the runoff by approximately 45° or had relative in-phase relationships at the annual timescale. Scattered inter-annual and interdecadal oscillations between the runoff and precipitation were observed before the 1990s at the Tangnaihai hydrological station, with complicated relative phase relationships. Evapotranspiration

ChinaXiv合作期刊

was the most important meteorological factor affecting the multiscale characteristics of the runoff at the Toudaoguai hydrological station. The difference was that the Toudaoguai hydrological station had a high PASC for the scattered semiannual oscillation period with a complicated phase relationship. However, an annual oscillation period between the runoff and evapotranspiration was found during 1956–1985 at the 95% significance level, with the runoff lagging behind the evapotranspiration by about 90° at the Toudaoguai hydrological station (Fig. 4c).

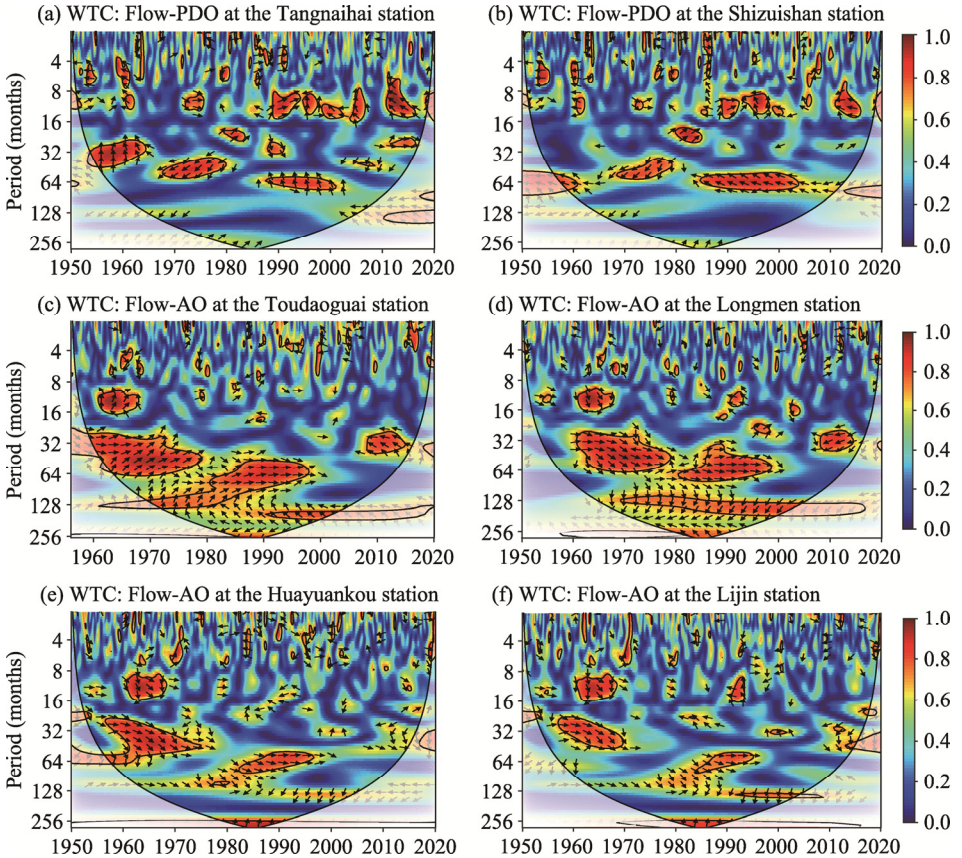

Fig. 3 Bivariate wavelet coherence (WTC) between the runoff and individual circulation factors at six hydrological stations. (a), Tangnaihai hydrological station; (b), Shizuishan hydrological station; (c) Toudaoguai hydrological station; (d), Longmen hydrological station; (e), Huayuankou hydrological station; (f), Lijin hydrological station. PDO, Pacific Decadal Oscillation; AO, Arctic Oscillation. Each driving factor can best explain the variations in the multiscale characteristics of the runoff for all of the circulation factors. The black semi-circular line is the cone of influence domain. The regions enclosed by the thick black contour lines indicate the 95% significance level. The directions of the arrows indicate the relative phase relationship between the two time series, with the positive phase pointing right and the negative phase pointing left.

The PASC was high between the runoff and temperature for the annual oscillation period before 2000 at the Longmen hydrological station, with the temperature leading the runoff by approximately 45° (Fig. 4d). The number of rainy days was the meteorological factor that can best explain the multiscale characteristics of the runoff at the Huayuankou station. A scattered annual oscillation period was observed throughout the study period, with a relative in-phase relationship. In addition, the PASC was relatively high during the 32- to 64-month oscillation periods at the 95% significance level during 1950–1970 and 1983–1993. Moreover, in the decadal oscillation period, from 1950 to 1993, the coherence was strong, with the number of rainy days leading the runoff by about 90° (Fig. 4e). At the Lijin hydrological station, precipitation was the main controlling factor explaining the multiscale characteristics of the runoff. Throughout the entire study period, the annual oscillation periods exhibited significant coherence, with the precipitation leading the runoff by about 45°. In addition, in the decadal period, the precipitation led the runoff by about 120° during the 1960s and 1980s (Fig. 4f).

chinaXiv:202109.00013v1

ChinaXiv合作期刊

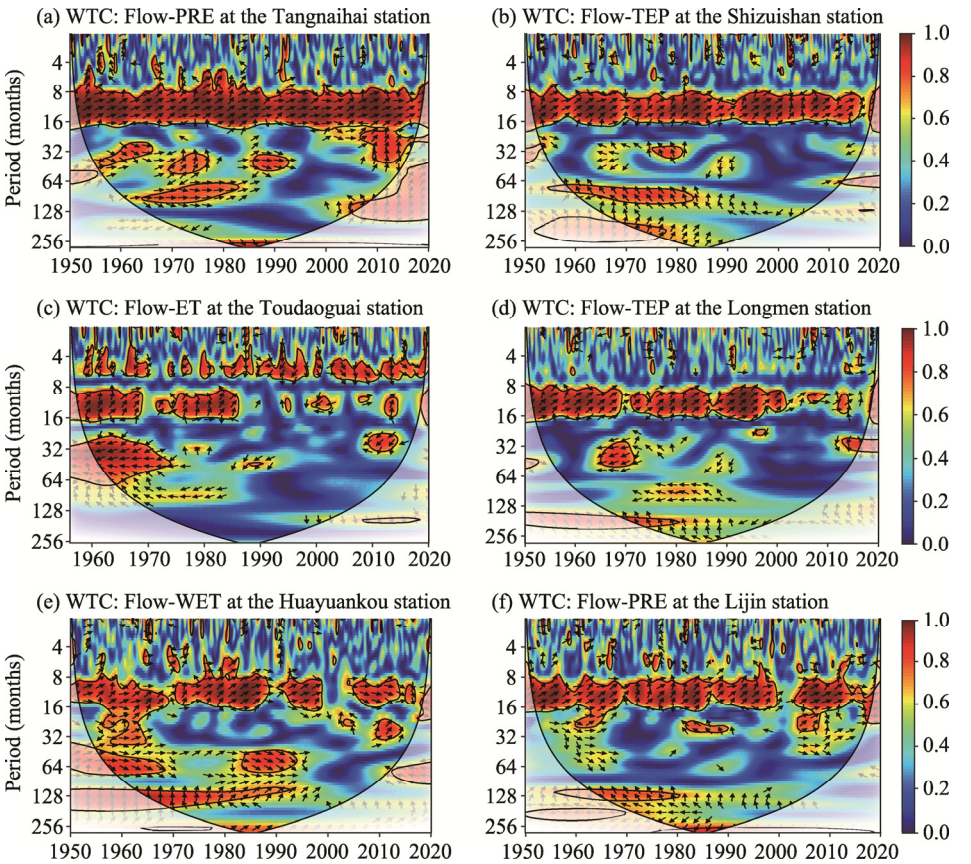

Fig. 4 WTC between the runoff and individual meteorological factors at six hydrological stations. (a), Tangnaihai hydrological station; (b), Shizuishan hydrological station; (c) Toudaoguai hydrological station; (d), Longmen hydrological station; (e), Huayuankou hydrological station; (f), Lijin hydrological station. PRE, precipitation; TEP, temperature; ET, evapotranspiration; WET, the number of rainy days. Each driving factor can best explain the variations in the multiscale characteristics of the runoff for all of the meteorological factors.

4.3 Synergistic effects of multiple factors on the runoff variations

4.3.1 Synergistic effects of two environmental factors

In fact, the multiscale characteristics of the runoff are generally affected by multiple factors (Chu et al., 2019). Table 4 lists the combinations of two factors (including combinations of two meteorological factors, two circulation factors, and a meteorological factor and a circulation factor) that can best explain the variations in the runoff.

Table 4 Multiple wavelet coherence (MWC) and PASC between the runoff and two combined factors

Station	Two factors	MWC	PASC (%)	Two factors	MWC	PASC (%)	Two factors	MWC	PASC (%)
TNH	AO-SOI	0.617	13.09	PRE-NAO	0.750	34.30	PRE-WET	0.755	36.90
SZS	AO-SOI	0.618	12.93	PRE-AO	0.701	21.85	PRE-WET	0.697	26.98
TDG	AO-PDO	0.639	15.44	PRE-AO	0.688	24.60	PRE-WET	0.671	23.32
LM	AO-PDO	0.648	13.65	PRE-AO	0.708	26.67	PRE-ET	0.683	20.62
HYK	AO-NAO	0.628	13.02	PRE-SOI	0.707	25.20	PRE-WET	0.713	25.18
LJ	AO-NAO	0.627	13.46	PRE-SOI	0.705	25.28	PRE-TEP	0.718	26.88

The average largest MWC and the PASC values of the two-factor combinations were higher than any of the single factor cases (Table 4). In terms of the combinations of two circulation factors, the AO and SOI, AO and PDO, and AO and NAO were each the best two-factor combination for two stations (Tangnaihai and Shizuishan for the combination of AO and SOI, Toudaoguai and Longmen

chinaXiv:202109.00013v1

ChinaXiv合作期刊

for the combination of AO and PDO, and Huayuankou and Lijin for the combination of AO and NAO). In addition, the AO was included in all of the optimal combinations of two circulation factors for explaining the multiscale characteristics of the runoff. The average largest MWC and PASC values of the combinations of two circulation factors were 0.630 and 13.60%, respectively. In terms of the influence of a single circulation factor on the runoff, the PDO was more predominant, and the PASC value was the highest compared to other circulation factors at the Tangnaihai and Shizuishan hydrological stations. However, the PDO was not in the combination with the largest PASC for these two hydrological stations. Part of the reason for this is that most of the areas with significant coherence between the runoff and PDO had already shown due to the effects of additional circulation factors on the runoff (Hu and Si, 2016; Nalley et al., 2019). The synergistic effects of two large-scale circulation variables on the multiscale characteristics of the runoff in different time-frequency domains were revealed by the MWC analysis (Fig. 5).

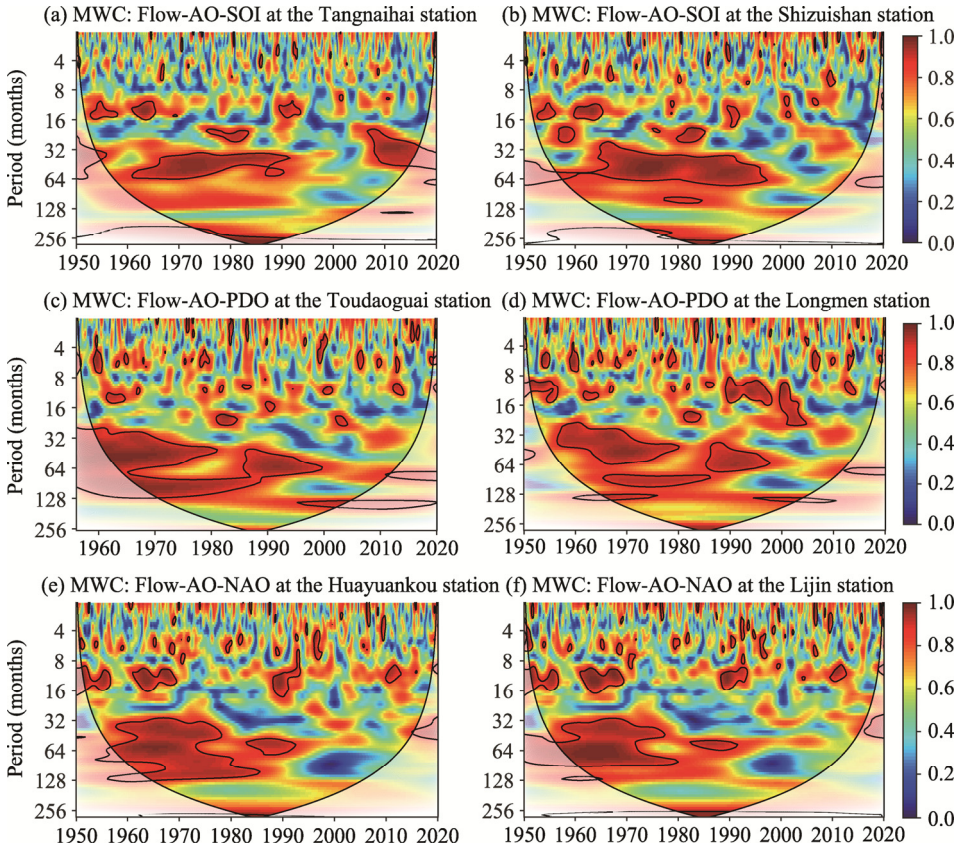

Fig. 5 Multiple wavelet coherence (MWC) between the runoff and combinations of two circulation factors at six hydrological stations. (a), Tangnaihai hydrological station; (b), Shizuishan hydrological station; (c) Toudaoguai hydrological station; (d), Longmen hydrological station; (e), Huayuankou hydrological station; (f), Lijin hydrological station. SOI, Southern Oscillation Index; NAO, North Atlantic Oscillation.

It was found that the combined effect of the AO and SOI on the runoff at the Tangnaihai and Shizuishan hydrological stations was relatively significant in the 32- to 64-month periods from 1960 to 1990. The AO and PDO was the optimal combination of two circulation factors for explaining the runoff variations at the Toudaoguai and Longmen hydrological stations. Moreover, for the significant coherence for the scattered semiannual and annual periodicities, the combined impact of the AO and PDO on the multiscale characteristics of the runoff was prominent. In particular, the significant 32- and 128-month periods were strong, potentially reflecting the low-frequency periods of the PDO (Nalley et al., 2019). The AO and NAO combination of two circulation factors could explain the runoff variations at the Huayuankou and Lijin hydrological

chinaXiv:202109.00013v1

ChinaXiv合作期刊

stations better, which is similar to the strong coherence relationship (Fig. 5) at these stations, with a 32- to 128-month scale from 1960 to 1980.

In this study, we also explored the synergistic effects of combinations of one meteorological factor and one circulation factor on the runoff variations (Fig. 6). The average largest MWC and PASC values of the combinations of one meteorological factor and one circulation factor were 0.71 and 26.32%, respectively. In addition, precipitation was included in all of the good combinations, which indicates that precipitation was the prominent factor affecting the multiscale characteristics of the runoff. The most common combinations were precipitation-AO and precipitation-SOI, which were respectively the optimal combinations for three and two hydrological stations (Shizuishan, Toudaoguai, and Longmen for the precipitation-AO combination, and Huayuankou and Lijin for the precipitation-SOI combination).

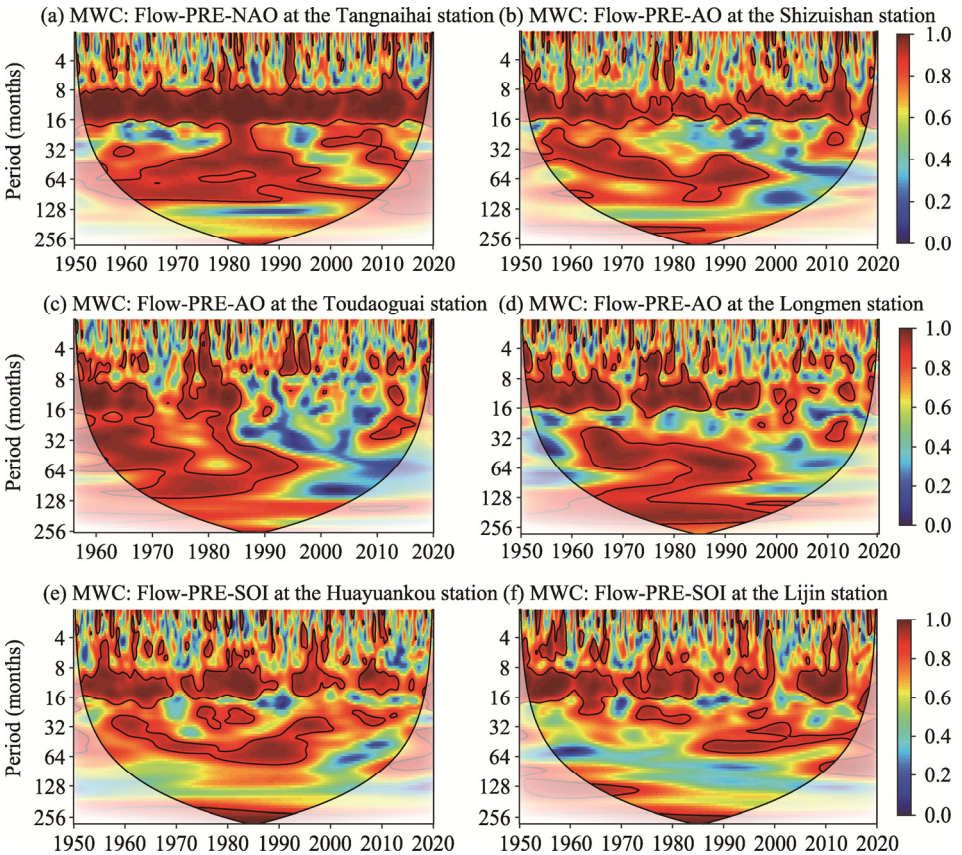

Fig. 6 MWC between the runoff and combinations of one meteorological factor and one circulation factor at six hydrological stations. (a), Tangnaihai hydrological station; (b), Shizuishan hydrological station; (c) Toudaoguai hydrological station; (d), Longmen hydrological station; (e), Huayuankou hydrological station; (f), Lijin hydrological station.

However, precipitation-SOI was the optimal combination of one meteorological factor and one atmospheric circulation factor that could explain the multiscale characteristics of the runoff at the Huayuankou and Lijin hydrological stations better (Fig. 6e and f). The lower YRB is adjacent to the western Pacific Ocean and has flat terrain, so ENSO events have a strong influence on the local- and regional-scale climate through ocean-atmosphere interactions, such as transporting moisture into the atmosphere and shifting the regional rainfall pattern in the YRB (Wang et al., 2006). Wang et al. (2006) also found that ENSO events are strongly associated with the low runoff at the Lijin hydrological station, which reasonably supports our findings.

We further investigated the impacts of combinations of two meteorological factors on the runoff variability (Table 4; Fig. 7). Similar to the combinations of one meteorological factor and

chinaXiv:202109.00013v1

ChinaXiv合作期刊

one circulation factor, precipitation was part of most of the optimal combinations of two meteorological factors. This further indicates that precipitation played a dominant role in the runoff variations. As can be seen from Tables 2 and 4, the average largest MWC of the combinations of two meteorological factors was 0.71, which is 0.25 higher than that for the individual meteorological factors. All of the PASC values of the combinations of two meteorological factors were higher than the WTC values of the individual meteorological factors (Table 3). In particular, the PASCs at the Shizuishan, Toudaoguai, Longmen, and Lijin hydrological stations increased by more than 5.00%, indicating that the runoff variability was controlled by multiple factors. According to the MWC results between the runoff and combinations of two meteorological factors (Fig. 7), the combined effects mainly regulate the runoff on small time scales, especially on the semiannual and annual scales.

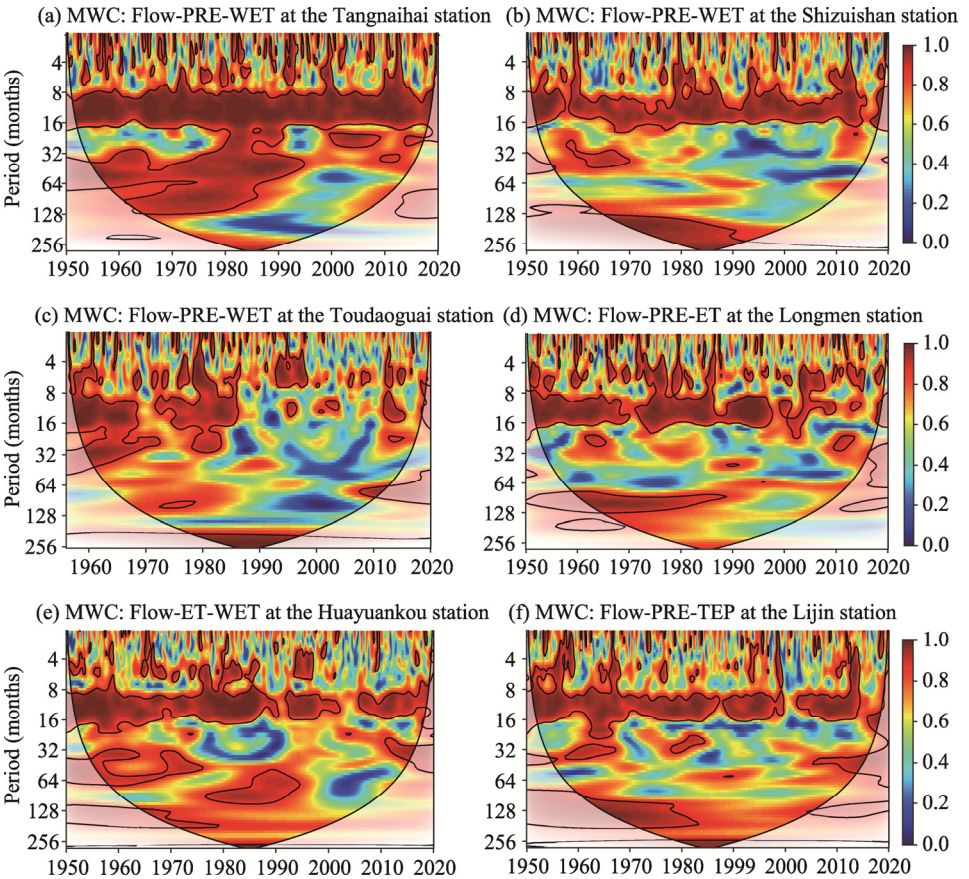

Fig. 7 MWC between the runoff and the combinations of two meteorological factors at six hydrological stations. (a), Tangnaihai hydrological station; (b), Shizuishan hydrological station; (c) Toudaoguai hydrological station; (d), Longmen hydrological station; (e), Huayuankou hydrological station; (f), Lijin hydrological station.

4.3.2 Synergistic effects of three environmental factors

Furthermore, we investigated the responses of the runoff variations to the combinations of three driving factors. All of the coherences were increased by more than 0.800 when three factors were used in the MWC analysis (Table 5). In terms of the combinations of two circulation factors and one meteorological factor, the average largest PASC and MWC were 26.63% and 0.834, respectively, and the number of rainy days, AO, and SOI combination was the dominant explanatory combination in the upper and middle reaches of the YRB. However, the optimal combination that could explain the runoff variations in the lower reaches of the YRB was precipitation-NAO-SOI. In fact, the two different optimal combinations had internal relevance to a certain extent mainly because precipitation and the number of rainy days are different

chinaXiv:202109.00013v1

ChinaXiv合作期刊

evaluation indices of the same atmospheric physical phenomenon. Moreover, the AO and NAO are similar in essence, both reflecting the strength of the mid-latitude westerly winds. The difference is that the horizontal scale of the AO is larger and the NAO is a representation of the AO in the North Atlantic region (Wallace, 2000). Many previous studies have documented the fact that the NAO and AO indices have a significant high correlation coefficient, and both have a vital influence on the climate anomalies in the middle and high latitude regions of Asia (Hurrell, 1996; Deser, 2000; Wallace, 2000).

Table 5 MWC and PASC between the runoff and combinations of three factors

Station	Three factors	MWC	PASC (%)	Three factors	MWC	PASC (%)	Three factors	MWC	PASC (%)
TNH	WET-AO-SOI	0.855	35.95	PRE-ET-AO	0.864	39.34	PRE-ET-WET	0.846	34.76
SZS	WET-AO-SOI	0.822	24.11	PRE-WET-AO	0.837	29.67	TEP-ET-WET	0.823	29.37
TDG	WET-AO-PDO	0.819	23.56	PRE-ET-NAO	0.884	26.86	PRE-TEP-ET	0.822	24.55
LM	WET-AO-SOI	0.837	29.09	PRE-WET-AO	0.832	25.86	PRE-TEP-ET	0.823	20.67
HYK	PRE-NAO-SOI	0.838	22.37	PRE-WET-AO	0.842	22.79	PRE-ET-WET	0.834	21.58
LJ	PRE-NAO-SOI	0.833	24.71	PRE-ET-AO	0.820	28.19	PRE-TEP-ET	0.835	22.41

As shown in Figure 8, the AO and SOI combined with the number of rainy days was the optimal combination of one meteorological factor and two circulation factors for explaining the runoff variations in the annual period with a high continuous coherence at the Tangnaihai and Shizuishan hydrological stations from 1950 to 2019. Significant inter-annual oscillations (mainly 3–5 a) occurred from 1965 to 1995 under the impacts of multiple factors at the Tangnaihai and Shizuishan hydrological stations. Furthermore, a scattered annual period with significant coherence was observed for four hydrological stations (Tangnaihai, Longmen, Huayuankou, and Lijin) in the middle and lower reaches of the Yellow River. Notably, the inter-annual periods (approximately 3–5 a) also had a strong significance under the combined impacts of multiple factors (WET, AO, and SOI) at the Longmen hydrological station.

Table 5 and Figure 9 summarize the combinations of two meteorological factors and one circulation factor that can explain the runoff variations in the YRB better. The average largest PASC and MWC were 28.79% and 0.847, respectively, which are higher than those of the combinations of one meteorological factor and two circulation factors. Moreover, precipitation and AO were both contained in all of the combinations, which is similar to the two-factor combinations in the MWC analysis. The combination of precipitation, number of rainy days, and AO, and the combination of precipitation, evapotranspiration, and AO were both dominant modes of the runoff variability in the YRB. Moreover, among all of the one-, two-, and three-factor combinations investigated in this study, the combinations of two meteorological factors and one circulation factor were the dominant mode in controlling the runoff variability, with the largest PASC and MWC. Compared with the combinations of three meteorological factors, although the individual meteorological factors had stronger effects on the runoff variability than any of the individual circulation factors, the combinations of three meteorological factors were not the best mode for explaining the runoff variations (Fig. 10), which is partly due to the strong collinearity among the meteorological factors (Hu et al., 2017). In simple terms, the runoff variations that are explained by additional factors on a certain time scale may have already been explained by the existing factors, and the overlapping effects weakened the ability of the additional factors to explain the runoff variability (Zhao et al., 2018). The MWC results of the combinations of two meteorological factors and one circulation factor are presented in Figure 9. Clearly, there was a continuous annual period from 1950 to 2019 at the Tangnaihai and Shizuishan hydrological stations. Notably, the combination of precipitation, evapotranspiration, and AO strongly controlled the runoff variations on 16- to 128-month time scales from 1970 to 1990 at the Tangnaihai hydrological station. Moreover, intermittent annual and semiannual periods with a high coherence were evident throughout the study period at the Toudaoguai, Longmen, Huayuankou, and Lijin hydrological stations.

chinaXiv:202109.00013v1

ChinaXiv合作期刊

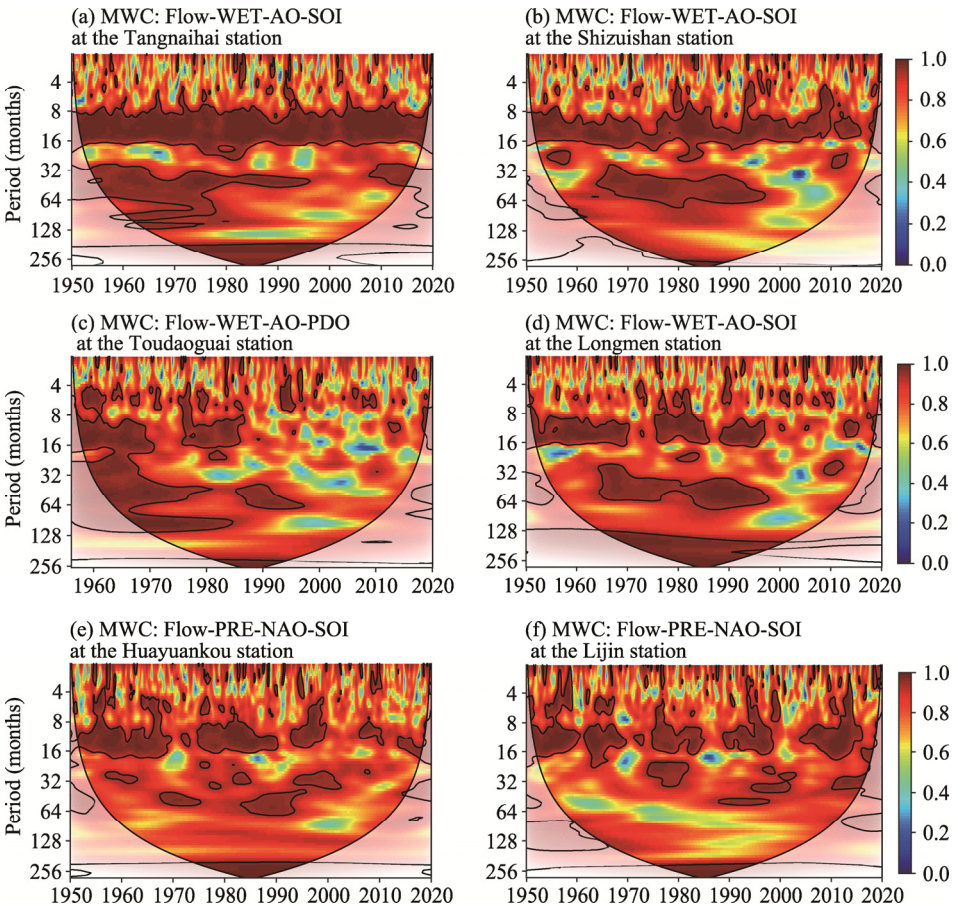

Fig. 8 MWC between the runoff and combinations of a meteorological factor and two circulation factors at six hydrological stations. (a), Tangnaihai hydrological station; (b), Shizuishan hydrological station; (c) Toudaoguai hydrological station; (d), Longmen hydrological station; (e), Huayuankou hydrological station; (f), Lijin hydrological station.

5 Discussion

5.1 Effect of human activities on the relationships between the runoff and various driving factors

The impact of human activities on the runoff variations is seasonal (Dai et al., 2009), and in this study, we focused on the multi-scale characteristics of the runoff on all time-frequency scales, which effectively abates the effects of human activities on the results, to a certain extent. However, the influence of human activities (e.g., reservoir and dam impoundment, water and soil conservation measures, and water intake and diversion) on the relationships between the runoff and different driving factors is still worth considering and discussing. Indeed, many previous studies have reported that human activities are a dominant factor for explaining the runoff changes in the YRB over the past five decades (Kong et al., 2016; Wang and Sun, 2020). The relevant soil and water conservation measures usually include afforestation, grass planting, and terrace construction (Kong et al., 2016). The indirect hydrological effect of land use changes on runoff variations has gradually increased over the last few decades (Li et al., 2020). Grass planting and afforestation directly enhance the vegetation coverage, thereby increasing the water storage capacity of the soil and enhancing rainwater infiltration (Wang et al., 2012; Kong et al., 2016), which indirectly affect the runoff generation mechanism. In addition, permafrost degradation caused by rising temperatures changes the land cover types, which further strengthens the indirect effects of the land cover on the runoff signature variations in the source

chinaXiv:202109.00013v1

ChinaXiv合作期刊

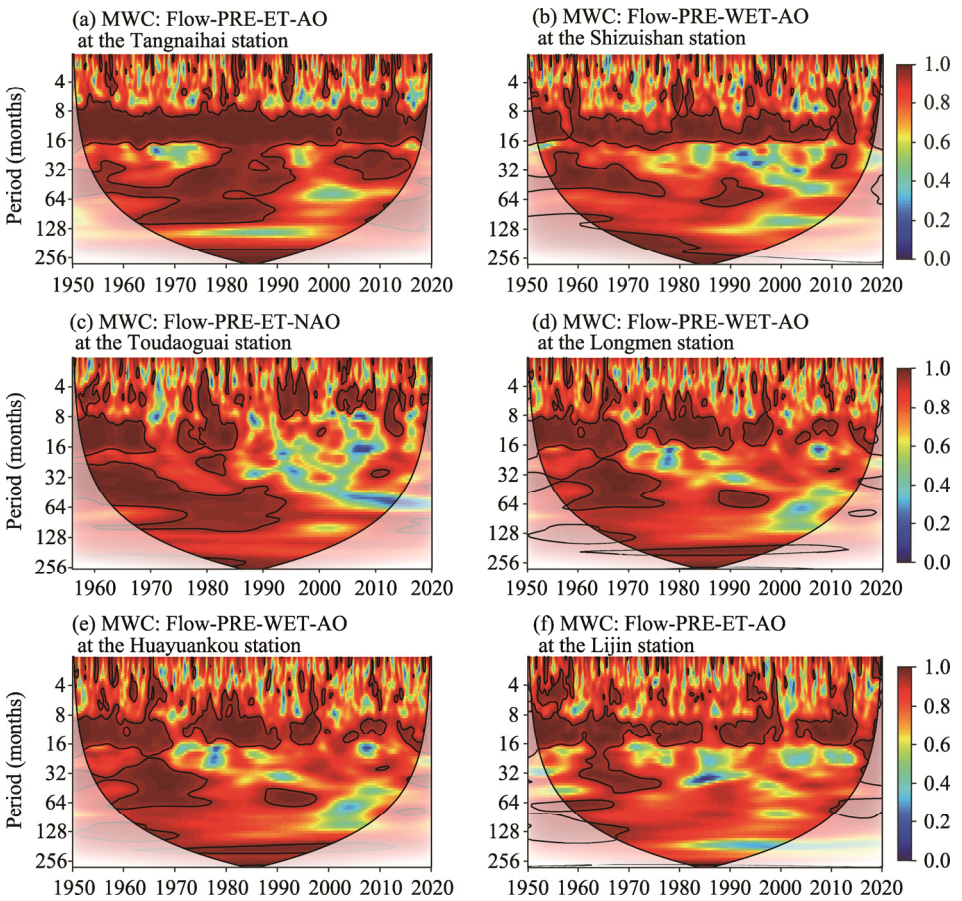

Fig. 9 MWC between the runoff and the combinations of two meteorological factors and one circulation factor at six hydrological stations. (a), Tangnaihai hydrological station; (b), Shizuishan hydrological station; (c) Toudaoguai hydrological station; (d), Longmen hydrological station; (e), Huayuankou hydrological station; (f), Lijin hydrological station.

region of the YRB (Wang et al., 2020). Through land terracing, the concentrated flow is greatly regulated by limiting the water available for runoff (Feng et al., 2020). However, the construction of dams and reservoirs is the most direct way to regulate the hydrological cycle among all human activities in river basins (Vörösmarty et al., 2003). In view of this, we further investigated the influence of human activities on the results of this study by taking the time of completion of four large reservoirs (the Longyangxia (1986), Liujiaxia (1968), Sanmenxia (1960), and Xiaolangdi (1999) reservoirs) on the mainstream of the Yellow River as key time nodes. The locations of the reservoirs are shown in Figure 1.

According to the wavelet power spectrum of the runoff, the oscillation intensity of the annual period scale at the Tangnaihai hydrological station did not change significantly throughout the study period (Fig. 2a). Mainly since the area above the Tangnaihai hydrological station is the source area of the YRB, the disturbance of the runoff caused by human activities is weak (Wang et al., 2012). The annual periodic oscillation intensity of the runoff at the Shizuishan hydrological station weakened after 1987, which was mainly due to the construction of the Longyangxia Reservoir above the Shizuishan hydrological station in 1986. This reservoir further strengthened the distribution and regulation of the runoff (Wang et al., 2006; Tian et al., 2019). However, according to the wavelet coherence analysis of the runoff and temperature at the Shizuishan hydrological station (Fig. 4b), it is obvious that the controlling effect of the reservoir on the runoff had a negligible impact on the relationships between the runoff and meteorological factors since the intensity of the annual common oscillation period was continuous throughout the

chinaXiv:202109.00013v1

ChinaXiv合作期刊

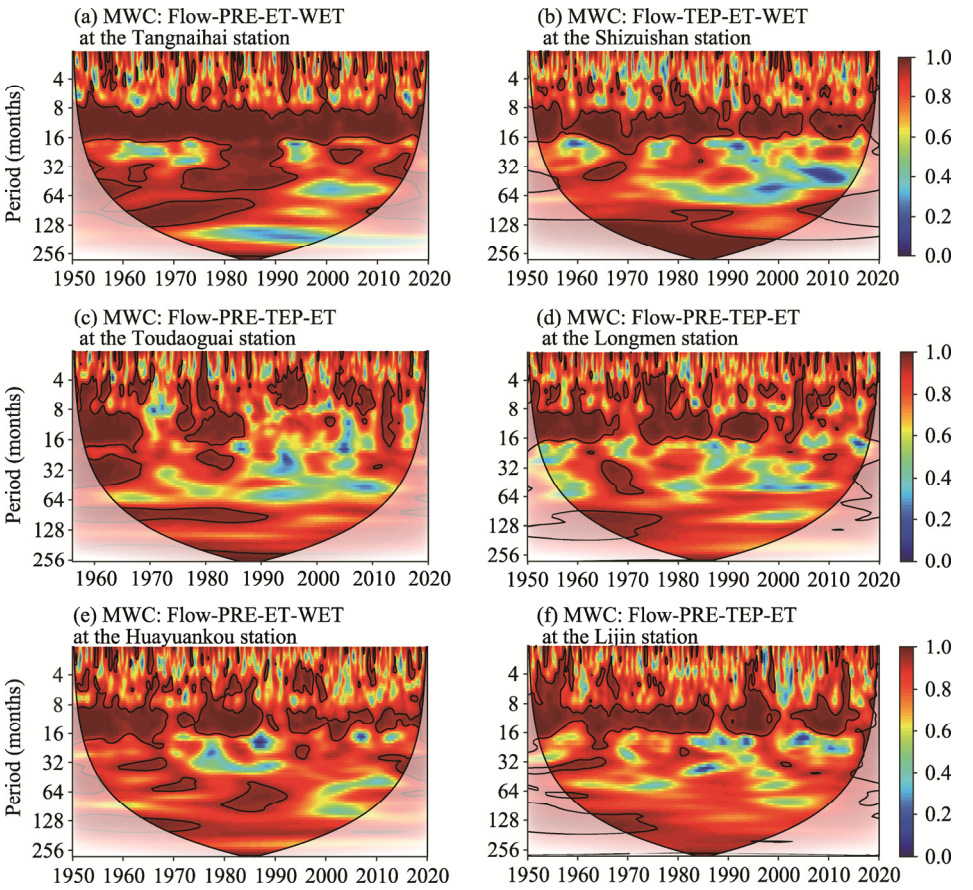

Fig. 10 MWC between the runoff and the combinations of three meteorological factors at six hydrological stations. (a), Tangnaihai hydrological station; (b), Shizuishan hydrological station; (c) Toudaoguai hydrological station; (d), Longmen hydrological station; (e), Huayuankou hydrological station; (f), Lijin hydrological station.

study period. Furthermore, based on the wavelet power spectrum and wavelet coherence spectrum of the runoff at the Toudaoguai and Longmen hydrological stations (Figs. 2 and 4), the semi-annual period scale of the runoff and the common coherence between the runoff and meteorological factors on the semi-annual and annual scales at both stations did not exhibit significant variations after the operation of the Longyangxia Reservoir.

Huayuankou and Lijin hydrological stations are located downstream of the Sanmenxia and Xiaolangdi reservoirs. There was almost no significant variation in the annual oscillation intensity of the runoff at the Lijin hydrological station. However, the wavelet power spectrum of the runoff at the Huayuankou hydrological station exhibited a progressive energy loss trend on the annual period scale after 1986 (Fig. 2e), which is consistent with the time at which the operation of the Longyangxia Reservoir began. In addition, the intensity of the wavelet coherence between the runoff and meteorological factors was almost continuous on the annual scale at the Huayuankou hydrological station, which indicates that the operation of the reservoirs did not seriously interfere with the identification of the fine structure of the runoff evolution conducted in this study.

5.2 How many factors are sufficient to explain the multiscale characteristics of the runoff?

Based on the results of this study, it was found that as the number of factors in the combination increases, the MWC also increases, whereas the PASC may not necessarily increase. Taking the Tangnaihai hydrological station as an example, the influence of four-factor combinations on the runoff was further analyzed (data were not shown), and it was found that the average MWC was 0.915. Although the value of the MWC increased, the rate of increase decreased as the number of combination factors increased. From one- to two-factor combinations, from two- to three-factor

chinaXiv:202109.00013v1

ChinaXiv合作期刊

chinaXiv:202109.00013v1

combinations, and from three- to four-factor combinations, the average rates of increase were 0.279, 0.148, and 0.060, respectively. However, the average PASC of the four-factor combinations was 29.14%, which is 7.54% lower than that of the three-factor combinations, which may be due to the increase in the PASC threshold for statistical significance after adding an additional factor (Ng and Chan, 2012). Therefore, in this study, we found that a combination of three-factors is sufficient to explain the variations in the multiscale characteristics of the runoff in the YRB. Furthermore, the meteorological factors directly affect the runoff, while the large-scale atmospheric circulation factors indirectly influence the runoff via hydrological or meteorological processes (Su et al., 2019). Consequently, the meteorological factors can explain the variations in the runoff in different time-frequency domains better. However, when all of the factors contained in a combination are meteorological factors, it is not necessarily the optimal combination for explaining the variations in the runoff. Part of the reason for this is that the overlapping effect caused by the collinearity among the factors reduces the variance contribution of some of the factors (Hu et al., 2017). Moreover, the ocean climate signals usually last for a long time due to the huge heat capacity of the ocean, which makes the potential predictability of large-scale circulation factors stronger (Gobena and Gan, 2009; Su et al., 2018). Therefore, combinations of large-scale circulation factors and meteorological factors are usually more reasonable for explaining the variations in the runoff on all time scales.

5.3 How do meteorological and circulation factors synergistically drive the runoff variations?

Numerous studies have investigated the relationship between the runoff and precipitation in various sections of the YRB. Liu and Cui (2011) showed that the response of the runoff to precipitation exhibits strong nonlinearity and is more sensitive in dry regions or years in the YRB. Li et al. (2012) explored the response of the runoff to climate change in the source region of the Yellow River, and their results revealed that rainfall is the dominant driver of the runoff in this region. In the middle reaches of the YRB, Zhao et al. (2014) found that there is a significant positive relationship between the runoff and precipitation, and there is a simultaneous decreasing trend from 1950 to 2010. Therefore, it makes sense that precipitation is contained in all of the optimal combinations. Moreover, the AO is one of the major features of the global climate system, as its regional counterpart, the North Atlantic Oscillation (NAO) (Gong et al., 2002), which mainly influences the precipitation and cyclonic activity in the high and mid-latitude regions of the Northern Hemisphere (Jones et al., 1997; Givati and Rosenfeld, 2013). In addition, owing to the enhancement of the polar night jet stream, the positive winter AO can not only prevent the cold air in the polar region from invading the high latitude regions of East Asia, leading to warm air advection from the North Atlantic to the high latitude regions of Europe, but also cause more precipitation in the high latitude regions of Eurasia (Thompson and Wallace, 2001). According to Gong and Wang (2003) and Park et al. (2011), the positive winter AO is associated with the positive precipitation anomalies over inland China, especially over central China (30°–40°N, east of 100°E). Therefore, it is reasonable that the combinations of precipitation-AO and precipitation-NAO can explain the runoff variations in the upstream and midstream reaches of the YRB better (Tangnaihai, Shizuishan, Toudaoguai, and Longmen hydrological stations). Furthermore, the global circulation factors mainly modulate the inter-annual to decadal oscillations in the runoff (Gobena and Gan, 2009), whereas the meteorological factors mainly control the seasonal and annual periods of the runoff. Therefore, the weak collinearity between the different types of driving factors means that the combination modes can synergistically explain the runoff variations on all timescales in the YRB better.

6 Conclusions

In this study, the multiscale characteristics of the runoff at the Tangnaihai, Shizuishan, Toudaoguai, Longmen, Huayuankou, and Lijin hydrological stations in the YRB were investigated using the CWT method. In addition, the WTC and MWC methods were used to

ChinaXiv合作期刊

investigate the synergistic effects and scale-dependent relationships between the runoff and various driving factors. The CWT results indicate that the runoff exhibited significant continuous or discontinuous annual oscillations during the study period at the Tangnaihai, Shizuishan, Huayuankou, and Lijin hydrological stations, while significant semiannual and annual periods occurred simultaneously with intermittent breaks at the Toudaoguai and Longmen hydrological stations. Scattered inter-annual time scales were also observed at all of the hydrological stations. The WTC results show that the meteorological factors can explain the runoff variations better than the atmospheric circulation factors. The AWC and PASC between the runoff and individual meteorological factors were 0.454 and 19.89%, respectively. Among all of the circulation factors investigated, the AO and PDO most significantly affected the multiscale characteristics of the runoff variations. The meteorological factors mainly affected the runoff on seasonal and annual time scales, whereas the atmospheric circulation factors mainly regulated the runoff on inter-annual and decadal time scales.

According to the MWC results, for the combined effects of two circulation factors, the AO-SOI, AO-PDO, and AO-NAO were each the optimal combination. The precipitation-AO and precipitation-SOI were the most common combinations of one meteorological factor and one circulation factor for explaining the runoff variations. Among all of the two- or three-factor combinations, the MWC analysis indicates that the precipitation-evapotranspiration (or the number of rainy days)-AO combination performed the best in terms of revealing the multiscale characteristics of the runoff in the YRB. The results of this study are conducive to understanding hydrology-climate interactions and to predicting the future trend of the runoff under changing atmospheric and oceanic conditions. Moreover, further study should be conducted to explore the nonlinear relationships between the runoff and additional atmospheric circulation factors.

chinaXiv:202109.00013v1

Acknowledgements

This research was financially supported by the National Natural Science Foundation of China–Shandong Joint Fund (U2006227, U1906234) and the National Natural Science Foundation of China (51279189).

References

Arthington Á H, Naiman R J, Mcclain M E, et al. 2010. Preserving the biodiversity and ecological services of rivers: new challenges and research opportunities. Freshwater Biology, 55(1): 1–16.

Chen L, Chang J X, Wang Y M, et al. 2019. The regional asymmetric effect of increased daily extreme temperature on the streamflow from a multiscale perspective: A case study of the Yellow River Basin, China. Atmospheric Research, 228: 137–151.

Cheng Q P, Zuo X A, Zhong F L, et al. 2019. Runoff variation characteristics, association with large-scale circulation and dominant causes in the Heihe River Basin, Northwest China. Science of the Total Environment, 688: 361–379.

Chu H B, Wei J H, Qiu J, et al. 2019. Identification of the impact of climate change and human activities on rainfall-runoff relationship variation in the Three-River Headwaters region. Ecological Indicators, 106: 105516, doi: 10.1016/j.ecolind.2019.105516.

Croley II T E, Hartmann H C. 1985. Resolving thiessen polygons. Journal of Hydrology, 76(3–4): 363–379.

Dai A G, Qian T T, Trenberth K E, et al. 2009. Changes in continental freshwater discharge from 1948 to 2004. Journal of Climate, 22(10): 2773–2792.

Deser C. 2000. On the teleconnectivity of the "Arctic Oscillation". Geophysical Research Letters, 27(6): 779–782.

Fang Z F, Bogena H, Kollet S, et al. 2015. Spatio-temporal validation of long-term 3D hydrological simulations of a forested catchment using empirical orthogonal functions and wavelet coherence analysis. Journal of Hydrology, 529: 1754–1767.

Feng J, Wei W, Pan D L. 2020. Effects of rainfall and terracing-vegetation combinations on water erosion in a loess hilly area, China. Journal of Environmental Management, 261: 110247, doi: 10.1016/j.jenvman.2020.110247.

Gerten D, Rost S, Bloh W V, et al. 2008. Causes of change in 20th century global river discharge. Geophysical Research Letters, 35(20), doi: 10.1029/2008GL035258.

Givati A, Rosenfeld D. 2013. The Arctic Oscillation, climate change and the effects on precipitation in Israel. Atmospheric Research, 132: 114–124.

ChinaXiv合作期刊

Gobena A K, Gan T Y. 2009. The role of Pacific climate on low-frequency hydroclimatic variability and predictability in southern Alberta, Canada. Journal of Hydrometeorology, 10(6): 1465–1478.

Gong D Y, Wang S W. 2003. Influence of Arctic Oscillation on winter climate over China. Journal of Geographical Sciences, 13(2): 208–212.

Gong G, Entekhabi D, Cohen J. 2002. A large-ensemble model study of the wintertime AO–NAO and the role of interannual snow perturbations. Journal of Climate, 15(23): 3488–3499.

Grinsted A, Moore J C, Jevrejeva S. 2004. Application of the cross wavelet transform and wavelet coherence to geophysical time series. Nonlinear Processes in Geophysics, 11: 561–566.

Hare S R, Mantua N J. 2000. Empirical evidence for North Pacific regime shifts in 1977 and 1989. Progress in Oceanography, 47(2–4): 103–145.

Hu W, Si B C. 2016. Multiple wavelet coherence for untangling scale-specific and localized multivariate relationships in geosciences. Hydrology and Earth System Sciences, 20(8): 3183–3191.

Hu W, Si B C, Biswas A, et al. 2017. Temporally stable patterns but seasonal dependent controls of soil water content: Evidence from wavelet analyses. Hydrological Processes, 31(21): 3697–3707.

Huo J Y, Liu C J, Yu X X, et al. 2020. Effects of watershed char and climate variables on annual runoff in different climatic zones in China. Science of The Total Environment, 754: 142157, doi: 10.1016/j.scitotenv.2020.142157.

Hurrell J W. 1996. Influence of variations in extratropical wintertime teleconnections on Northern Hemisphere temperature. Geophysical Research Letters, 23(6): 665–668.

Jevrejeva S, Moore J, Grinsted A. 2003. Influence of the Arctic Oscillation and El Niño‐Southern Oscillation (ENSO) on ice conditions in the Baltic Sea: The wavelet approach. Journal of Geophysical Research: Atmospheres, 108(D21), doi: 10.1029/2003JD003417.

Jones P D, Jónsson T, Wheeler D. 1997. Extension to the North Atlantic Oscillation using early instrumental pressure observations from Gibraltar and south-west Iceland. International Journal of Climatology: A Journal of the Royal Meteorological Society, 17(13): 1433–1450.

Kong D X, Miao C Y, Wu J W, et al. 2016. Impact assessment of climate change and human activities on net runoff in the Yellow River Basin from 1951 to 2012. Ecological Engineering, 91: 566–573.

Koopmans L. 1974. The Spectral Analysis of Time Series. New York: Academic Press, 119–164.

Labat D, Ababou R, Mangin A. 2000. Rainfall–runoff relations for karstic springs. Part II: continuous wavelet and discrete orthogonal multiresolution analyses. Journal of Hydrology, 238(3–4): 149–178.

Labat D. 2008. Wavelet analysis of the annual discharge records of the world's largest rivers. Advances in Water Resources, 31(1): 109–117.

Labat D. 2010. Cross wavelet analyses of annual continental freshwater discharge and selected climate indices. Journal of Hydrology, 385(1–4): 269–278.

Li B F, Shi X, Lian L S, et al. 2020. Quantifying the effects of climate variability, direct and indirect land use cover change, and human activities on runoff. Journal of Hydrology, 584: 124684, doi: 10.1016/j.jhydrol.2020.124684.

Li H Z, Zhang Q, Singh V P, et al. 2017a. Hydrological effects of cropland and climatic changes in arid and semi-arid river basins: a case study from the Yellow River basin, China. Journal of Hydrology, 549: 547–557.

Li L, Shen H Y, Dai S, et al. 2012. Response of runoff to climate change and its future tendency in the source region of Yellow River. Journal of Geographical Sciences, 22(3): 431–440.

Li Z W, Xu X L, Xu C H, et al. 2017b. Monthly sediment discharge changes and estimates in a typical karst catchment of southwest China. Journal of Hydrology, 555: 95–107.

Liu F, Chen S L, Dong P, et al. 2012. Spatial and temporal variability of water discharge in the Yellow River Basin over the past 60 years. Journal of Geographical Sciences, 22(6): 1013–1033.

Liu Q, Cui B S. 2011. Impacts of climate change/variability on the streamflow in the Yellow River Basin, China. Ecological Modelling, 222(2): 268–274.

Liu Y M, Lu M M, Yang H J, et al. 2020. Land–atmosphere–ocean coupling associated with the Tibetan Plateau and its climate impacts. National Science Review, 7(3): 534–552.

Mantua N J, Hare S R, Zhang Y, et al. 1997. A Pacific interdecadal climate oscillation with impacts on salmon production. Bulletin of the American Meteorological Society, 78(6): 1069–1080.

Montaldo N, Sarigu A. 2017. Potential links between the North Atlantic Oscillation and decreasing precipitation and runoff on a Mediterranean area. Journal of Hydrology, 553: 419–437.

Murgulet D, Valeriu M, Hay R R, et al. 2017. Relationships between sea surface temperature anomalies in the Pacific and Atlantic Oceans and South Texas precipitation and streamflow variability. Journal of Hydrology, 550:726–739.

chinaXiv:202109.00013v1

ChinaXiv合作期刊

Nalley D, Adamowski J, Biswas A, et al. 2019. A multiscale and multivariate analysis of precipitation and streamflow variability in relation to ENSO, NAO and PDO. Journal of Hydrology, 574: 288–307.

Ng E K, Chan J C. 2012. Geophysical applications of partial wavelet coherence and multiple wavelet coherence. Journal of Atmospheric and Oceanic Technology, 29(12): 1845–1853.

Niedzielski T, Szymanowski M, Miziński B, et al. 2019. Estimating snow water equivalent using unmanned aerial vehicles for determining snow-melt runoff. Journal of Hydrology, 578: 124046, doi: 10.1016/j.jhydrol.2019.124046

Nijssen B, O'Donnell G M, Hamlet A F, et al. 2001. Hydrologic sensitivity of global rivers to climate change. Climatic Change, 50(1–2): 143–175.

Notarnicola C. 2020. Hotspots of snow cover changes in global mountain regions over 2000–2018. Remote Sensing of Environment, 243: 111781, doi: 10.1016/j.rse.2020.111781.

Park T W, Ho C H, Yang S. 2011. Relationship between the Arctic Oscillation and cold surges over East Asia. Journal of Climate, 24(1): 68–83.

Peng J, Chen S L, Dong P. 2010. Temporal variation of sediment load in the Yellow River basin, China, and its impacts on the lower reaches and the river delta. Catena, 83(2–3): 135–147.

Piao S L, Friedlingstein P, Ciais P, et al. 2007. Changes in climate and land use have a larger direct impact than rising CO_2 on global river runoff trends. Proceedings of the National Academy of Sciences, 104(39): 15242–-15247.

Shen Q N, Cong Z T, Lei H M. 2017. Evaluating the impact of climate and underlying surface change on runoff within the Budyko framework: A study across 224 catchments in China. Journal of Hydrology, 554: 251–262.

Shi H L, Hu C H, Wang Y G, et al. 2017. Analyses of trends and causes for variations in runoff and sediment load of the Yellow River. International Journal of Sediment Research, 32(2): 171–179.

Su L, Miao C Y, Borthwick A G, et al. 2017. Wavelet-based variability of Yellow River discharge at 500-, 100-, and 50-year timescales. Gondwana Research, 49: 94–105.

Su L, Miao C Y, Kong D X, et al. 2018. Long-term trends in global river flow and the causal relationships between river flow and ocean signals. Journal of Hydrology, 563: 818–833.

Su L, Miao C Y, Duan Q Y, et al. 2019. Multiple-wavelet coherence of world's large rivers with meteorological factors and ocean signals. Journal of Geophysical Research: Atmospheres, 124(9): 4932-4954.

Sun Q H, Miao C Y, AghaKouchak A, et al. 2016. Century-scale causal relationships between global dry/wet conditions and the state of the Pacific and Atlantic Oceans. Geophysical Research Letters, 43(12): 6528 – 6537.

Thompson D W, Wallace J M. 1998. The Arctic Oscillation signature in the wintertime geopotential height and temperature fields. Geophysical Research Letters, 25(9): 1297–1300.

Thompson D W, Wallace J M. 2001. Regional climate impacts of the Northern Hemisphere annular mode. Science, 293(5527): 85–89.

Tian S M, Xu M Z, Jiang E H, et al. 2019. Temporal variations of runoff and sediment load in the upper Yellow River, China. Journal of Hydrology, 568: 46–56.

Torrence C, Compo G P. 1998. A practical guide to wavelet analysis. Bulletin of the American Meteorological society, 79(1): 61–78.

Trenberth K E. 1997. The definition of El Niño. Bulletin of the American Meteorological Society, 78(12): 2771–2778.

Vörösmarty C J, Meybeck M, Fekete B, et al. 2003. Anthropogenic sediment retention: major global impact from registered river impoundments. Global & Planetary Change, 39(1–2): 169–190.

Wallace J M. 2000. North atlantic oscillatiodannular mode: Two paradigms—one phenomenon. Quarterly Journal of the Royal Meteorological Society, 126(564): 791–805.

Wang H, Sun F B. 2020. Variability of annual sediment load and runoff in the Yellow River for the last 100 years (1919–2018). Science of The Total Environment: 143715, doi: 10.1016/j.scitotenv.2020.143715.

Wang H J, Yang Z S, Saito Y, et al. 2006. Interannual and seasonal variation of the Huanghe (Yellow River) water discharge over the past 50 years: connections to impacts from ENSO events and dams. Global and Planetary Change, 50(3–4): 212–225.

Wang J J, Shi B, Pan X Y, et al. 2020. Multi-scale characteristics of precipitation and its relationship with ENSO and AO. Journal of Coastal Research, 104(SI): 23–28.

Wang S, Fu B J, Piao S L, et al. 2016. Reduced sediment transport in the Yellow River due to anthropogenic changes. Nature Geoscience, 9(1): 38–41.

Wang S J, Yan M, Yan Y X, et al. 2012. Contributions of climate change and human activities to the changes in runoff increment in different sections of the Yellow River. Quaternary International, 282: 66–77.

Wang S P, Zhang Z Q, McVicar T R, et al. 2012. An event-based approach to understanding the hydrological impacts of

chinaXiv:202109.00013v1

ChinaXiv合作期刊

different land uses in semi-arid catchments. Journal of Hydrology, 416: 50–59.

Wang W, Zhang Y Y, Tang Q H. 2020. Impact assessment of climate change and human activities on streamflow signatures in the Yellow River Basin using the Budyko hypothesis and derived differential equation. Journal of Hydrology, 591(7401): 125460, doi: 10.1016/j.jhydrol.2020.125460.

Wei W, Chang Y P, Dai Z J. 2014. Streamflow changes of the Changjiang (Yangtze) River in the recent 60 years: Impacts of the East Asian summer monsoon, ENSO, and human activities. Quaternary International, 336: 98–107.

Wine M L, Zou C B. 2012. Long-term streamflow relations with riparian gallery forest expansion into tallgrass prairie in the Southern great plains, USA. Forest Ecology and Management. 266, 170–179.

Wu D, Yan D H, Yang G Y, et al. 2013. Assessment on agricultural drought vulnerability in the Yellow River basin based on a fuzzy clustering iterative model. Natural hazards, 67(2): 919–936.

Wu L Y, Zhang X, Hao F H, et al. 2020. Evaluating the contributions of climate change and human activities to runoff in typical semi-arid area, China. Journal of Hydrology, 590: 125555, doi: 10.1016/j.jhydrol.2020.125555

Wu Y N, Gan T Y, She Y T, et al. 2020. Five centuries of reconstructed streamflow in Athabasca River Basin, Canada: Non-stationarity and teleconnection to climate patterns. Science of The Total Environment, 746: 141330, doi: 10.1016/j.scitotenv.2020.141330

Wu Y Y, Fang H W, Huang L, et al. 2020. Changing runoff due to temperature and precipitation variations in the dammed Jinsha River. Journal of Hydrology, 582: 124500, doi: 10.1016/j.jhydrol.2019.124500

Xu K H, Milliman J D, Xu H. 2010. Temporal trend of precipitation and runoff in major Chinese Rivers since 1951. Global and Planetary Change, 73(3–4): 219–232.

Yang W T, Long D, Bai P. 2019. Impacts of future land cover and climate changes on runoff in the mostly afforested river basin in North China. Journal of Hydrology, 570: 201–219.

Yellow River Conservancy Commission of the Ministry of Water Resources. 2001–2019. Yellow River Sediment Bulletin. Zhengzhou: Yellow River Conservancy Commission of the Ministry of Water Resources. (in Chinese)

Zhao G J, Tian P, Mu X M, et al. 2014. Quantifying the impact of climate variability and human activities on streamflow in the middle reaches of the Yellow River basin, China. Journal of Hydrology, 519: 387–398.

Zhao R Y, Biswas A, Zhou Y, et al. 2018. Identifying localized and scale-specific multivariate controls of soil organic matter variations using multiple wavelet coherence. Science of The Total Environment, 643: 548–558.

chinaXiv:202109.00013v1